The role of eddies in determining the structure and response of the wind-driven Southern Hemisphere overturning: Initial results from the Modeling Eddies in the Southern Ocean Project

Robert Hallberg

Anand Gnanadesikan

NOAA Geophysical Fluid Dynamics Lab, Princeton, NJ 08542

Manuscript in preparation for Journal of Physical Oceanography

10/8/2004

Contact e-mail: Robert.Hallberg@noaa.gov

Abstract

It has been proposed that winds and eddies within the Southern Ocean play an important role in determining the density structure of the global ocean and the magnitude and structure of the global thermohaline overturning. The Modeling Eddies in the Southern Ocean (MESO) project was designed to examine this hypothesis. Sensitivity studies to test this picture were performed with a hemispheric isopycnal-coordinate circulation model with realistic geometry and idealized forcing at a range of resolutions from relatively coarse (2^o) to eddy-permitting ($1/6^o$). In our model, the great bulk of density transformation occurs within the surface layers. As we move from coarse to fine resolution we see effects of eddies on both the mean structure of the overturning and the response of the overturning to changes in surface winds. While the presence of resolved eddies does not greatly alter the qualitative picture of the ocean circulation developed over the years, it does result in some significant differences. In particular, eddies play an important role in the overturning cell involving the transformation of dense bottom waters and light tropical waters to intermediate waters. In the presence of resolved eddies, the upper branch of this cell extends southwards by hundreds of kilometers and the lower branch draws on comparatively lighter deep waters. The response of this cell to changes in the surface winds is also sensitive to the presence of eddies. In non-eddying simulations changing the Ekman transport produces comparable changes in the overturning, much of it involving transformation of deep waters and resembling the mean circulation. In eddy-permitting simulations a significant fraction of the response is compensated by eddy-induced transport drawing from lighter waters, differing

significantly from the mean circulation. This significant difference calls into question the ability of coarse-resolution ocean models to accurately capture the impact of changes in the Southern Ocean on the global ocean circulation.

1. Introduction

The oceans play a critical role in determining global climate, insofar as they transport heat from the tropics to polar regions and help determine the distribution of sea ice (Winton, 2003). It is a matter of some interest, therefore, how the ocean would respond to climate change. A particular unknown in this respect is the role of mesoscale eddies. With scales ranging from a few km in high latitudes to a few hundred along the equator (Stammer, 1998), energetic mesoscale eddies are well known to play a vital role in lateral tracer dispersion (Ledwell et al., 2000). However, until recently, many analytical theories of the global ocean circulation have focused on the large-scale planetary geostrophic circulation and largely neglected the effect of eddies. Important examples of this genre include Huang and Pedlosky (1999) and Talley (2002). These theories have focused on the circulation of the wind-driven gyres, in which information is conveyed by large-scale, baroclinic waves.

However, there is one part of the ocean where eddies are known to play a major role in the dynamics, namely the Southern Ocean (Johnson and Bryden, 1989; Marshall et al., 1993; Bryden and Cunningham, 2003; Marshall and Radko, 2003). In most of the ocean, momentum input from surface winds to the light surface waters can be balanced by piling up these light waters against a continent (Veronis, 1996). This means that the wind-driven circulation can largely be limited to the surface layers. However, the Southern Ocean contains a band of latitudes where there is no continuous topography above a depth of around 1800m. Strong winds in this band drive a northward Ekman transport. In order for the mass budget to be closed, this northward flow must be supplied

by southward-flowing waters. However, the equations of motion place some strong constraints on such flows. Above the depth of the ridges, geostrophic flow averaged along a level surface must be zero. Thus while the mass budget demands a southward flow, the momentum budget apparently demands that this flow occur at depth, below the depths of ridges.

. There are two limiting options by which these two flows can be connected to each other. One option is that the southward-flowing dense water upwells, is converted into Antarctic Surface Waters as a result of freshwater input and flows northwards in the Ekman layer (Warren et al., 1996; Toggweiler and Samuels, 1998; Doney et al., 2000; Gnanadesikan and Hallberg, 2000; Speer et al., 2001) . Such a picture requires substantial watermass transformation, but does not require any process to flux momentum downwards in the water column. The second option is that baroclinic eddies, spawned by the Antarctic Circumpolar Current, act to transfer momentum downwards in the water column (Johnson and Bryden, 1989; Marshall et al., 1993; Gille, 1997; Tansley and Marshall, 2001). To the extent that the stress at the bottom of a given density layer is the same as the stress at the top of that layer there is then no stress divergence and thus no net flow. In this limit *no* watermass transformation is required. In the real ocean, both processes are likely to play a role (Gnanadesikan, 1999; Hallberg and Gnanadesikan, 2001). As shown in Figure 1, which shows a schematic of the circulation within the Southern Ocean, the northward Ekman flux will likely have a component due to upwelling deep water and a component due to the supply of lighter water (shown by the wavy arrows) associated with eddies.

In large-scale general circulation models of the type used in climate studies, the effect of mesoscale eddies is often parameterized in terms of a diffusive tracer flux along isopycnals (Redi, 1982; Griffies et al., 1998) and an advective flux resulting from a diffusive smoothing of isopycnal depths (Gent and McWilliams, 1990; Gent et al., 1995; Visbeck et al., 1997). Both of these processes are governed by a lateral diffusion coefficient, which is often taken to be the same (Griffies, 1998). Gnanadesikan (1999) proposed that one could represent the deep upwelling flux in Figure 1 as a difference between the northward Ekman flux and the eddy driven upwelling flux, and proposed the following closure for these fluxes

$$T_{upw} = T_{ek} - T_{eddy} = \frac{\tau L_x}{\rho f} - \frac{A_I D L_x}{L_y} \qquad (1)$$

where τ is the wind stress, L_x is the distance along a latitude circle, ρ is the density, f is a scale value for the Coriolis parameter, A_I is a lateral eddy diffusion coefficient (which may itself be a strong function of the ocean state, but is often taken as constant), D is the depth of the pycnocline and L_y is the north-south length scale over which the pycnocline shoals. Within this picture increasing A_I would increase the fraction of northward-flowing water in the Ekman layer drawn from light water. In general this would be expected to increase the mean temperature of the southward flowing water and thus the heat transport to the Southern Ocean (Gnanadesikan et al., 2003). The impact of eddies is thus to increase the amount of thermohaline overturning that occurs in light waters. What the conceptual model does not tell us, however, is which water masses will be transformed, what the pathways of transformation will be, and the relationship between A_I and the large-scale density structure.

Similarly, though this model suggests that increasing the wind stress τ will increase the overturning and watermass transformation, without a closure for A_I (and a comprehensive theory for D) we do not know how much the overturning will change and what watermasses will supply it. Hallberg and Gnanadesikan (2001) showed that in a two-layer model there are three separate regimes of response. At low levels of eddy energy, changes in T_{ek} produced changes in T_{upw} but not T_{eddy}. At moderate levels, changes in T_{ek} were accompanied by changes in both T_{upw} and T_{eddy} such that the fraction of flow supplied by the two sources was almost constant. At high eddy energy levels, changes in T_{ek} were almost completely supplied by T_{eddy}. This paper noted an interesting effect in which increasing the winds increased the eddy energy, resulting in a tendency toward localized homogenization of potential vorticity over ridges and in their lee in the lower layer of the model. This meant that as the winds increased the path of the current became increasingly affected by the topography.

In order to explore these issues more fully, we initiated a modeling study entitled Modeling Eddies in the Southern Ocean (MESO). This study was designed to explore the following questions

-What is the structure of the diapycnal overturning circulation in the Southern Ocean?

-What is the role of eddies in determining this structure?

-How does this overturning circulation change in response to changing forcing?

-How does the eddy field change in response to changing forcing?

-How do these local changes project onto the global overturning circulation?

-To what extent can we represent this response without fully resolving the eddies?

Answering the final question in particular is critical for assessing the extent to which the coarse-resolution models used in climate change studies can accurately characterize the response to changing forcing. This paper describes the first round of MESO simulations and presents initial results.

2. Methods

a.) Physical model

The model used for these simulations is the isopycnal model of Hallberg (1995). We use an isopycnal model for a number of reasons. First, fewer vertical degrees of freedom are required to represent internal wave modes and realistic topography relative to a level-coordinate model. Second, analysis of the model is much easier in watermass space- the space used by observational physical oceanographers to discuss ocean circulation. Third, the cascade of variance to small scales does not lead to nonphysical diapycnal mixing, as is likely in a Z-coordinate model with vigorous eddies (Griffies et al., 2000).

The model solves the primitive equations in constant density layers. A three-way time-split (barotropic, baroclinic, diabatic/tracer) with subcycling of the shorter time steps assures that the model can be integrated efficiently while conserving momentum, mass and tracers (by layer), potential vorticity, and energy (Arakawa and Hsu, 1990). A monotonic, conservative tracer advection algorithm (based on Easter, 1993) is used. The full nonlinear equation of state is used, following Sun et al. (1999). The model allows for turbulent entrainment in descending overflows and other regions of small resolved shear Richardson number, using the scheme of Hallberg (2000), but a weak diapycnal

diffusivity of 10^{-5} m^2 s^{-1} elsewhere in the interior. The 20 interior layers were chosen to provide a reasonable resolution across the density range of the southern ocean and a limited resolution of the light water structure at low latitudes.

A three-layer bulk mixed layer (Hallberg, 2003) is used. The mixed layer depth is determined by an energy budget, following a long tradition starting with Kraus and Turner (1967). This mixed layer is then divided into two sublayers, which are well-mixed with respect to tracers but not with respect to velocity, allowing for shear-driven restratification. In addition, a parameterized restratifying circulation is also introduced to the mixed layer based on the horizontal density gradients (Hallberg, 2003), to account for the fact the viscous restratification would occur predominantly at smaller horizontal wavelengths than are resolved (Young, 1994). As described by Hallberg (2003) in the absence of this shear-driven restratification mixed layer depths become excessively deep. A buffer layer below the mixed layer allows fluid to detrain smoothly into the interior (Thompson et al., 2002).

The low-resolution model runs (2º and 1º) use the equivalent of the Gent and McWilliams (GM, 1990) eddy parameterization. Runs were made with a GM coefficients varying between 0 and 2000 m^2/s. Only the runs with values of 0 and 1000 are presented here, but the cited tendencies are consistent with those from the broader range. The GM parameterization has the effect of flattening isopycnals. The higher resolution models (1/2º, 1/4º, and 1/6º) have no such parameterization. One run was made with the 1/2º model with GM to evaluate the impact of replacing the eddies with a parameterized representation of their effects. The biharmonic Smagorinsky viscosity of Griffies and

Hallberg (2000) is used to provide a momentum closure, removing enstrophy at small scales without substantially affecting the large-scale dynamics.

b.) Experimental design

MESO consists of a series of simulations at different horizontal resolutions (2º, 1º, 1/2º, 1/4º and 1/6º). MESO covers the entire Southern Hemisphere with a Mercator grid, so that the north-south resolution increases as we move poleward so as to keep boxes square. Thus at 60ºS the 1/2º model has a grid spacing of 27.8 km, while the 1/6º resolution is 9.3 km. Topography was generated using the dataset of Smith and Sandwell (1997) averaged to the grid resolution. All resolutions thus can be said to have "realistic" topography, though clearly the highest-resolution cases are the most accurate.

Boundary conditions at the northern boundary were handled by applying strong sponges with a restoring time scale that is short in comparison with the Atlantic crossing time of the first internal-mode equatorial Kelvin wave. The equator was chosen to be the northern boundary as it represents the only latitude where it is possible to specify density fields without specifying normal velocities (away from the equator, geostrophy dictates that density fields and velocity fields are strongly linked). Using strong sponges means that the mean state of the model is constrained to remain close to the real world and ensures that much of the spinup occurs in less than 20 years. It also ensures that changes in the Southern Ocean circulation are driven by local changes and not because of drifts caused by inaccurate watermass formation in the North Atlantic. However, it does mean that insofar as changes in wind stresses would be expected to eventually produce

significant changes in the pycnocline depth thoughout the global ocean (McDermott, 1996; Toggweiler and Samuels, 1998; Gnanadesikan and Hallberg, 2000) such changes are prevented. Weak sponges are applied around the Antarctic ice shelves to ensure the formation of Antarctic Bottom Water. While the details of these Antarctic shelf sponges can influence the formation rates of Antarctic Bottom Water and even the net transport of the ACC (through the thermal wind relationship starting from a very weak flow at the bottom), low-resolution test simulations with differing specifications for these sponges show very similar changes in response to the wind stress changes, which is the focus of this paper.

The models are forced for 20 years in a spinup period and for 20 years during the main experiment. During each period the wind stress is kept fixed (there is no seasonal cycle). The baseline wind stress produces the Ekman flux shown in Figure 3. The flux peaks at around 46ºS with a northward transport of 55 Sv.

A significant effort was made to come up with plausible buoyancy fluxes for the Southern Ocean. Existing reanalysis products are only loosely constrained by the few observations. By contrast, the sea-surface temperature and salinity are relatively well observed and so may be used to diagnose heat and salt fluxes. However, too strong a restoring has the effect of damping out eddy variability, since the temperature and salinity climatologies have only large-scale variability. An adaptive procedure for diagnosing the ocean heat and fresh water fluxes is described in Appendix A. This scheme allows for the fluxes to adjust to the circulation during the spinup period, while keeping the model near the climatological surface temperature and salinity. In the zonal mean, the surface heat fluxes are relatively small and plausible (Fig. 2), and the implied meridional heat

transport is within the range that can be deduced from atmospheric reanalyses and satellite observations (Trenberth and Caron, 2001). However, some aspects of the exact spatial distribution (such as a very large heat loss from the East Australia Current Extension) are not entirely plausible.

After the spinup period, the buoyancy forcing was fixed [apart from a weak feedback of temperature anomalies on the heat fluxes of 20 $Wm^{-2}K^{-1}$ and an equivalent weak feedback on surface salinity, and three separate runs were started. 20 $Wm^{-2}K^{-1}$ is a plausible feedback of heat fluxes on SST anomalies, based on bulk formulae. In one, (referred to as the middle winds) the wind stress is left unperturbed. Two other cases were started in which the wind stress was increased by 20% (referred to as the high winds case) or decreased by 20% (referred to as the low winds case). This is equivalent to a peak change in the Ekman transport of about 11 Sv. Recent work (see for example Renwick, 2004) suggests that winds over the Southern Ocean may have increased by about this amount during the last 25 years. The fact that the forcing remains constant (there is no annual cycle) ensures that all variability is intrinsic to the model. It also allows us to assess changes in the eddy field and the mean circulation in a statistically meaningful way using shorter runs.

It is helpful to put these simulations in the context of other fine-resolution studies of the Antarctic such as the Fine Resolution Antarctic Model (FRAM, Stevens and Ivchenko, 1994; Killworth and Nanneh, 1994) and the "quarter-degree" model of Semtner and Chervin (1992) used by Gille (1995) to examine the momentum balance of the Southern Ocean. Using the same terminology that we use, the Semtner-Chervin model would be a 0.4º model and FRAM would be a 1/2º model. Thus our 1/4º model is

run at twice the resolution of FRAM and our 1/6º model is at 3 times the resolution. Our spinup at high resolution is much longer than the spinups in either of these models. The Semtner and Chervin (1992) model was initialized from a 1/2º simulation and run for 5 years. FRAM was run for 20 years. Computationally, our highest resolution model represents 50 times the computation of FRAM. More recent simulations have been carried out at higher horizontal resolutions than FRAM (see for example Best et al., 1999; Zhang and Semtner, 2001), at a nominal resolution of ¼º (still coarser than our finest-resolution simulation) but a detailed study of the response of the flow to changes in surface forcing in such models has not been done.

3. Results

One of the standard diagnostics of a simulation of the Southern Ocean is the transport of the Antarctic Circumpolar Current though Drake Passage. Time series of this quantity are shown in Figure 4 at different resolutions. The observed transport varies between 110-150 Sv (Whitworth et al., 1982; Cunningham et al. 2003). The simulations tend to lie on the high side of this number, but are substantially lower than the 200 Sv found in the simulation of Semtner and Chervin (1992) and the 0.5° FRAM simulation of Killworth and Nanneh (1994). Refining horizontal resolution results in a decrease in the transport as eddies become increasingly energetic. The transport stabilizes after a few years in both the spinup and the perturbation runs. The 1° runs which include parameterized eddy effects are able to match the mean transport, and to a lesser extent the sensitivity of the mean transport seen in the ¼° runs. However, when the runs are

examined in detail, it can be seen that the separation between high, medium, and low wind stress cases that is so clear in the low-resolution (1° and ½°) simulations is much smaller and less clear in the 1/6° simulations. The response of the current to changes in winds when eddies are represented explicitly is significantly smaller than when they are parameterized. Simulations done with different values of A_I show roughly the same range in the response of the Drake Passage transport to wind changes despite having very different mean transports. The Drake Passage transport response is likely to be difficult to capture exactly without simulating the eddies directly.

The inclusion of eddies results in very large variability in Drake Passage transport on short time scales (Figure 4b) even though the forcing is steady. The variability has large amplitude (peak-to-trough range of 30 Sv) and occurs on a range of timescales. The ½° run with GM suppresses most of this variability, indicating that it is truly a function of the presence of eddies rather than being due to the resolution.

The eddy energy can be assessed by comparing the RMS sea surface height variability with altimeter data (Figure 5). The model captures the large scale features in the data, including the high variability off of South Africa associated with the shedding of Agulhas eddies, the southward trend of variability associated with the Southern Drift of the ACC, the extension of the variability to the north around Campbell Plateau and the high-variability region off of Argentina. Additionally the model captures some mid-latitude features such as the extension of high SSH variability off Queensland, Australia into the ocean interior. Detailed quantitative comparisons can be somewhat misleading, as our model has no variability in the forcing, while the TOPEX data reflects such forcing leading to much greater SSH variability in regions of low eddy activity. The 1/6° model

(5b,d) shows little change between the last five years of the spinup and the last five years of the experiment period with the same winds, indicating the eddy field is in rough equilibrium. The 1/6° model is somewhat more energetic than the ¼° model, particularly in energetic boundary current regions. The difference is not large, and a zonal average of the squared SSH anomalies shows that in the Southern Ocean the 1/6° model is about 30% more energetic than the ¼° model, but a factor of 3 more energetic than the ½° model.

Another signature of these differences can be seen in snapshots of the surface speed (Figure 6). The overall structure of the two fields is very similar, but the 1/6° model shows clear evidence of eddies at all locations. Particularly noticable in these simulations are the closed rings associated with Agulhas eddy shedding and the loops in the East Australian, and Brazil Currents. Animations of these simulations show these loops moving southward along the coast until they reach a separation point at which they drift into the interior. In the interior, the high-resolution simulations show that the current breaks down into individual jets, as found by Rhines (1977) and Panetta and Held (1982) in idealized simulations of geostrophic turbulence. As in the idealized simulations of Hallberg and Gnanadesikan (2001) these jets appear to form downstream of topography and then disappear as the current moves around such features as the Kerguelen and Campbell Plateaus and Drake Passage. Away from the boundary currents, there is also a clear sense of smaller scales (too small to be seen clearly in this hemispheric view) appearing as one moves to higher latitudes, consistent with changes in the internal deformation radius.

The overturning streamfunction in density space contains three principal cells (Figure 7). The green line approximately shows the densest water found in the mixed layer, so that any flow above this line is occurring partially in the mixed layer. Below this line, flow in the vertical can either be due to diapycnal mixing or to changes in the volume of particular layers. The flow shows many of the same features as the conceptual outline in Figure 1, but with one major difference - that there is a strong flow of light surface waters into the Southern Ocean. In the 1° model (Figure 7a) approximately 15 Sv of light water crosses a latitude of 40°S. Most of this water is rapidly transformed into Subantarctic Mode Water. Below this we see a cell in which about 18 Sv of North Atlantic Deep Water and Common Deep Water upwell into the mixed layer, where it is transformed into Antarctic Intermediate Water. Below this there is a strong cell by which Circumpolar Deep Waters are transformed into Antarctic Bottom Waters. Note that the great bulk of the watermass transformation occurs on density surfaces that are in or near the mixed layer (above the green line).

The circulation at 1/6° resolution has a similar qualitative structure (Figure 7b) as the 1° solution. To some extent this is reassuring, as it indicates that the coarse models do have some skill in simulating the large-scale circulation within the Southern Ocean. The cell involving the NADW and AAIW is very similar in the two models, and is in fact slightly stronger in the 1/6° model. The major difference is that the surface cell extends much further to the south. Whereas in the 1° model only 5 Sv of light surface water cross 44°S and mostly are converted to AAMW by 50°S, in the 1/6º model more than 10 Sv cross 44°S, half of which reaches a latitude of 58°S! This is the oceanic equivalent of the wintertime cold air outbreaks described by Held and Schneider (1999) in their

characterization of the isentropic overturning of the atmosphere. This contrast in the overturning circulation is also reflected in the diagnosed mean heat transport (Fig. 2b), with a significantly greater poleward heat transport in these latitudes in the 1/6º model. As in the 1º model this flow is likely entirely to be found within the mixed layer. It consists of outbreaks of warm surface water which are carried by eddies almost to the polar front.

It is noteworthy that in neither of these plots do we see the overturning streamfunction feature known as the Deacon Cell. This feature is ubiquitous in level-coordinate model simulations, and involves a northward transport in the surface layers, strong downwelling to the north of Drake Passage, southward transport in Drake Passage below the depths of the ridges, and strong upwelling to the north of Drake Passage. Doos and Webb (1994) argued that this feature was an artifact of averaging in the horizontal, as a stack of tilted flows along isopycnals could give the impression of a large diapycnal flow where none existed. They did not, however, find complete cancellation possibly because the FRAM model was not as well spun up. Our model does largely show a cancellation of the Deacon cell, though interestingly, this is only the case when the mixed layer is remapped into density space. When the mixed layer is separated from the interior waters there is a clear Deacon cell in those layers which outcrop- and the magnitude of this cell is hundreds of Sv! This emphasizes the degree to which the overturning circulation in the Southern Ocean is very much a three-dimensional structure.

It is perhaps counterintuitive that the surface cell has a net southward transport of the lightest waters even in latitudes (50°S-30°S) where the Ekman transport is northward. This is true even in the 1° model. In the coarse resolution model, this cell corresponds to

a southward transport of warm water in boundary currents and entrainment of this water into the ACC, where it cools and flows northward in the interior Ekman layer. This highlights the danger of thinking about the Circumpolar Current region in purely two-dimensional terms.

In the high-resolution model, coherent eddies carry warm waters much further polewards (up to 60°S), so that the lightest water is moving southwards throughout the entire Circumpolar band. Figure 8 shows a breakdown of the flow of this light water into time-mean and transient eddy components at 55°S and 60°S integrated over longitude. While the mean flow does bring light water into the Southern Ocean, most of this light water is returned in northward-flowing mean currents, especially at 60°S. The net transport is dominated by transient eddies. As seen in Fig. 8, at 60°S roughly 4 Sv of the lightest flow are due to transient eddies, while 1.2 Sv is due to the mean flow. Some of this eddy transport is the result of surges in the boundary currents, while some is broadly distributed across the Pacific

We now consider in more detail the changes in the simulation induced by changing the surface winds. As we have already seen, changing the surface winds has a relatively negligible effect on the Drake Passage transport (Figure 4). The largest impact is seen in the 1° model, with changes up to 8 Sv relative to a mean of 165 Sv (less than 5%). The 1/6° run shows much smaller and less consistent changes. Taken together, the runs show that a wind stress change of 20% produces a transport change of around 3-5%. Consistent with the small change in transport, the zonal mean sea surface height also shows very little change as a result of the change in wind stress (Figure 9a). The changes are only a few cm out of the 2 m drop across the ACC. This small response is consistent

with arguments put forward by Marshall et al. (1993) that the ACC should accelerate until it is baroclinically unstable. It is important to remember, however, that the damping of the density at the equator means that the mechanism for changing Drake Passage transport outlined in Gnanadesikan and Hallberg (2000) (namely an increase in the depth of the warm water sphere) has limited applicability in these simulations. Even were the damping not used, it is unlikely there would be a significant response within the limited time frame covered by these runs.

The eddy field, by contrast, has a much more linear response to changes in wind stress. Figure 9b illustrates that increasing the wind stress increases the mean square SSH variability and decreasing the wind stress decreases the SSH variability within the core of the ACC. The shape of the change is consistent with the baseline SSH variability. The change from increasing the winds by 20%, decreasing the winds by 20% and half the difference of the extreme cases lie on top of each other. Together this suggests a linear response of the eddy energy to wind stress. Such a response was also found in Hallberg and Gnanadesikan (2001). It is consistent with a simple balance in which eddy kinetic energy dissipation goes as E/T (where E is the energy and T is a scale time for dissipation) and eddy kinetic energy generation is proportional to $\vec{\tau} \cdot \vec{u}$ where $\vec{\tau}$ is the wind stress and $\vec{u}$ the surface velocity. Since, as was already noted, $\vec{u}$ is roughly constant, if T is also constant $E \sim \|\vec{\tau}\|$.

Many regions where the eddy kinetic energy changes (Figure 10) are associated with boundary currents or topographic features. There is an increase in the eddy energy off of Madagascar, Tasmania, the North Island of New Zealand, Campbell Plateau, where the ACC goes over the mid-Pacific ridge and in the Brazil Current. Not all places,

however, where the eddy energy is high exhibit an increase in eddy kinetic energy. For example the Agulhas retroflection does not show a strong increase in eddy kinetic energy. In general, the largest changes in EKE are found at the Subantarctic Front, rather than at the polar front lying further south. Similarly, off Kerguelen Plateau the eddy kinetic energy is high, but does not change significantly with increases in the winds.

What about the overturning streamfunction? As can be seen from Figure 3 the response from changing the winds by 20% would be to change the peak zonally-integrated Ekman transport by around 11 Sv. Figure 11 shows the response of the 1° model to increasing the winds. Both the surface/mode water and deep/intermediate cells increase. The surface cell increases by about 20%. The intermediate cell increases by about 35% (up to 7Sv out of ~20). South of about 40°S, the middle overturning cell accounts for the bulk of the change. Of the 7Sv change, 5 Sv comes from water denser than 1036.8, nominally dense Lower Circumpolar Deep Water. In the 1° model, a large fraction of the change in Ekman transport is supplied from deep upwelling.

The 1/6° simulation is qualitatively similar to the 1° simulation in that the dominant response is an intensification of the top two cells. The degree of intensification is quite different however. While the shallow cell intensifies by about 20% as in the 1° simulation, the changes in the deep/intermediate cell are noticeably weaker than in the 1° run. This can be seen more clearly in Figure 12, which shows the overturning streamfunction change vs. density for three different resolutions at 30°S, 40°S and 50°S.

The change in the deeper overturning cell (the conversion of deep waters into intermediate) is substantially smaller at the higher resolutions. At the peak, the deep response to increased winds is roughly 4.5 Sv at 1/6° resolution, compared to over 7 Sv at

1°. This result is systematic and robust. It appears for both strengthening and weakening winds. The ¼° resolution is clearly intermediate between the 1° and 1/6° resolutions, reflecting the presence of eddies, but at a lower intensity than in the higher resolution model. Moreover, although 15-year averages are shown in Fig. 12, the same trends appear in every pentad.

There is an asymmetry between the cases with the strengthening and weakening winds, in which the weakening winds show less difference between resolutions. The asymmetry is evident in both the magnitude of the overturning changes, and in the depth at which the changes occur. For figure. 12c, the increase in the deep cell overturning is 3.6 Sv for increased winds compared with 5 Sv for weakening winds. This asymmetry is consistent with the idea that eddies act to limit the shears, and as they become stronger they are increasingly able to compensate for forcing changes, as illustrated in the idealized study of Hallberg and Gnanadesikan (2001).

The deep (southward flowing) overturning response is systematically occurring in lighter, shallower waters at the higher resolutions. This can be clearly seen in the density-space overturning presented in Fig. 12c, which has a smaller range of density in its vertical axis, but it is clearly present in 12a and 12b as well. In this figure, there is almost a 4 Sv change in the southward flow of waters denser than 1037 in the 1° model, but none at higher resolutions. If we recast the overturning in “nominal depth” space (using the average depth of the isopycnal surface as the vertical coordinate instead of potential density) the results are even more dramatic (Figure 12d). As eddies are resolved the response of the overturning circulation is concentrated on shallower isopycnals. This is consistent with the idea, shown graphically in Fig. 1 (adopted from Speer et al. (2000)),

that eddies allow for mass fluxes above the level of topography which can feed a significant portion of the surface Ekman flux.

It is useful to contrast this behavior with that of the overturning associated with the wind-driven subtropical gyres. At 30°S the response of the upper cell (corresponding to the wind-driven gyres) is hardly affected by the model resolution. This suggests that eddies will have a relatively small direct impact on tropical heat transport associated with the wind-driven gyres. This is consistent with coarse-resolution studies (such as Gnanadesikan et al., 2003) which show that changing the lateral eddy mixing coefficient has a large effect on the transport of heat across the Southern Ocean, a moderate effect on the transport of heat between the Southern and Northern Hemispheres, but a minor impact on the export of heat from the tropics.

In summary, we have shown that resolving eddies can significantly alter the circulation of the Southern Ocean and its response to changes in forcing. Resolving eddies produces changes in the transport and variability of the ACC, results in extending the flow and transformation of light subtropical waters much further south, attenuates the response of the overturning circulation to changes in wind stress and results in the surface Ekman flow being fed from much shallower depths. Since this Ekman flow feeds interior flows of water that penetrate into the low latitudes, Southern Ocean eddies thus can have global effects.

4. Discussion

One important question upon which these results have some bearing is the role of surface winds in driving the global overturning circulation. There are currently two strains of discussion regarding how the overturning is driven- both largely based on circulation models at various levels of idealization. In the picture of Bryan (1987), Klinger and Marotzke (1999) and Klinger et al (2003) it is low-latitude diffusion that closes and drives the circulation. As pointed out by Huang (1999) the difference has important implications for modeling climate, since diffusion is driven by breaking internal waves which are not themselves modeled in GCMs. By contrast, a number of papers have found that Southern Ocean winds (Toggweiler and Samuels, 1993, 1998; Gnanadesikan, 1999; Gnanadesikan and Hallberg, 2000; Nof , 2000; Toggweiler and Bjornsson, 2001; Gent et al., 2001), temperatures (Vallis, 2000), eddies (Gnanadesikan, 1999; Gnanadesikan et al., 2003), and topography (Toggweiler and Samuels, 1995; Vallis, 2000) can play an important role in controlling the global stratification. This alternate view relies on the interior diffusion playing a relatively minor role.

MESO does not provide a clean test of the two views of circulation – since the strong sponges at the equator can either be interpreted as standing in for tropical diffusion within the pycnocline *or* surface transformation in the Northern Hemisphere. However, MESO does have implications for the question of the role of surface wind stress in driving the global overturning circulation. Certain papers (Marshall et al., 1993; Tansley and Marshall, 2001) suggest a limiting case in which changes in winds are locally compensated by changes in eddy fluxes without changing watermass transformation rates or large-scale circulation. Hallberg and Gnanadesikan (2001) found a similar limiting case when the eddy flux was much larger than the buoyancy-driven overturning. They

argued, however, that in the real ocean the two fluxes were likely of comparable size- so that an increase in the Ekman flux would be compensated by both an increase in watermass transformation and an increase in eddy flux. The present work supports the picture that both eddies and overturning transport changes balance changes in the winds.

It should be noted that several recent observational analyses differ substantially from the picture in which there are large fluxes of AAIW and SAMW out of the Southern Ocean. Where we find close to 20 Sv of AAIW formation from denser waters, an inverse model by Ganachaud and Wunsch (2000) finds only 8-9 Sv of net conversion. Sloyan and Rintoul (2001), also using an inverse model find only 3Sv. Iinterestingly, they also find very little net production of waters in AAIW classes within the Southern Ocean. Talley (2002) finds essentially no conversion of shallow waters to light waters within the Southern Ocean. In her circulation schematic, the 8 Sv of SAMW flowing northward across 30S is basically completely fed by southward flowing surface waters. This synthesis also shows essentially no net northward flow of AAIW-class waters- the roughly 10 Sv being produced in the Atlantic and Pacific being largely balanced by southward flows in the Indian Ocean. It is worth asking whether the neglect of the eddy processes responsible for the extension of the surface cell can account for this apparent discrepancy between models and integrated analyses of data.

A second area for which these results have important implications relates to whether it is important to resolve ocean eddies in order to understand climate change. One of the things that is most important for models to be able to resolve is the oceanic transport of heat. Smith et al. (2000) showed that a high-resolution simulation of the North Atlantic (1/10º resolution) in a level-coordinate model did a much better job at

getting the observed heat transport in the North Atlantic correct than previous models at lower resolution. However, it is unclear how much of this "improvement" was due to increased effective diapycnal diffusivity resulting from the cascade of tracer variance to small scales (Griffies et al., 2000). We see relatively small differences between the mean states' heat transports at different resolutions- implying that the degree to which the model is *adiabatic* is at least as important as the resolution of eddies for simulating the Southern Ocean heat transport. The difference in response to changes in wind stress between the 1º run with parameterized eddies and the 1/6º run with explicit eddies does suggest, however, that the details of eddy dynamics can play an important role in the magnitude of the response of the climate system to *changes* in forcing. In other words, while it may be possible to tune models to get the certain aspects of the current state of the ocean correct, it will be much more difficult to reproduce changes due to eddy activity.

5. Conclusions

It has long been known that eddies must be of leading order importance in the Southern Ocean momentum balance, and that the world ocean is largely filled by watermasses that originate or are eroded in the Southern Ocean (Sverdrup et al., 1942).. These two insights have led to two apparently contradictory views of how the circulation in the Southern Ocean is closed. As described in the introduction, the diabatic view highlights the role of water mass transformations in linking dense sourthward subsurface flows to the northward Ekman transport, while the adiabatic view emphasizes the role of

eddies in moving momentum downwards in the water column. Our results indicate that both pictures correctly describe key aspects of the circulation. There is a substantial Southern Ocean overturning circulation in the sense indicated by the diabatic view even in the presence of eddies. However the diabatic response to changes in wind forcing is substantially attenuated by the action of a vigorous eddy field as suggested by the adiabatic view.

The diabatic fluxes of water in our models are huge- more than 20 Sv of NADW is converted to AAIW and more than 30 Sv of thermocline water to SAMW. While the lack of a seasonal cycle may be important in determining the realism of these transformations, it should be clear that the Southern Ocean mixed layer has the potential to be a major region of watermass transformation. Transient eddies play an important role in this transformation – a role that is not well described by at least one common diffusive eddy parameterization (Gent and McWilliams, 1990). In the simulations shown here, they extend the cell which transforms light surface water to intermediate water far to the south (essentially to the polar front). This implies that the ocean could give up heat to the atmosphere even in latitudes where deep waters are being transformed into warmer AAIW and SAMW, and where the surface Ekman transport is northward.

Although many aspects of the mean circulation are qualitatively similar in the low resolution (parameterized eddy) simulations and the high resolution (eddy-rich) simulations, the response of these two models to wind stress changes are markedly different. The explicit eddies lead to a substantially lighter, shallower, and weaker change in the density-space overturning than in the coarse-resolution model. Other measures of

the circulation change, such as the Drake Passage transport, show a consistently smaller response with explicit eddies.

The eddy parameterizations used in the coarse resolution simulations shown here are of approximately the right strength to given the correct eddy impact on the mean state. However, with this effective tuning, they appear to dramatically underpredict the eddy response to changed forcing. It is not clear that these eddy effects can be effectively parameterized – they are nonlocal in both cause and effect, and strongly dependent on details of the flow structure.

None of the simulations presented here are numerically converged with respect to the eddies. However, the changes with increasing resolutions are consistent, and it is reasonable to expect that the numerically converged (infinite resolution) solutions would exhibit even stronger differences from the coarse resolution simulations than those shown here.

This study has examined a climatically interesting response only to wind forcing. It is not clear whether the eddy impact on the response to buoyancy forcing changes will be similar, but this is a question that should be examined.

Most importantly, this study emphasizes that it is imperative the oceanographic community develop and use accurate high resolution models to examine the response of the climate system. The changes shown here would be of import for a number of climatically relevant processes, including heat transport and storage, and carbon storage in the interior. Given that the Southern Ocean has been relatively underobserved and has seen dramatic changes in its forcing in recent years, the Southern Ocean response to the changing forcing is critical to understand if we are to correctly interpret the observations

currently being made to diagnose even the mean circulation of that critical part of the ocean. Finally, it is critical that climate predictions be assessed with the assistance of high resolution ocean models to ensure the validity of these predictions.

Acknowledgements: We thank the Geophysical Fluid Dynamics Laboratory, in particular our director Ants Leetmaa, for supporting the MESO project. Isaac Held, Robbie Toggweiler, Steve Griffies, and Geoff Vallis made important contributions to our design of this project.

Appendix A: Forcing the model

Suppose that the surface temperature tendency equation is written schematically as

$$H\, c_p \frac{\partial \theta}{\partial t} = M + \lambda(\theta_{Obs} - \theta) + F \qquad \text{(A.1)}$$

where M is the model tendency without forcing, λ is an effective damping rate (perhaps chosen to keep the model near data or perhaps from the bulk formulae), $H\, c_p$ is an effective (and as the mixed layer thickness H is not uniform, unknown) heat capacity, and F is an as yet unknown forcing rate. The long term mean balance for a perfect model with perfect observations in a steady state would be simply $M + F = 0$. F is unknown, and might be diagnosed by slowly adjusting the mean flux to make it compensate for the damping term

$$\frac{\partial F}{\partial t} = \gamma\lambda(\theta_{Obs} - \theta) \qquad \text{(A.2)}$$

where γ is a positive definite inverse damping timescale. F is now a prognostic variable of the model. The steady state of these equations (A.1) and (A.2) occurs when $\theta=\theta_{Obs}$

and $M+F = 0$. The unsteady behavior of these equations gives a damped oscillator with the desired final state.

Unfortunately, the results from using these equations in the model are absurd. The model admits spatial structures with much finer scales than are present in the mean state inferred from the observational datasets, and there are modest differences in the model's preferred location of a current compared with the observations. The result is enormous diagnosed fluxes with very small spatial scales.

Instead, a much more plausible diagnosed forcing can be obtained by using

$$\frac{\partial F}{\partial t} = \gamma\lambda(\theta_{Obs} - \theta) + \gamma L^2 \nabla^2 F \qquad \text{(A.3)}$$

where L is a length scale below which model-observation differences are not significant. The equations are still a damped oscillator, but now the steady state is given by

$$M + F - L^2 \nabla^2 F = 0 \qquad \text{(A.4a)}$$

$$\theta = \theta_{Obs} + (L^2 / \lambda)\nabla^2 F \qquad \text{(A.4b)}$$

At large scales compared with L, the Laplacian of the forcing is small, and the model is forced to agree with the observations. At small scales, the diagnosed forcing does not respond to model-observation discrepancies. At these smaller scales, anything but a full coupled model is likely to be wildly inaccurate because of the strong interactions between the two boundary layers. Thus, placing a lower cutoff on the scales where the restoring operates would seem to reduce the spurious impact on the dynamics, and this was chosen for this study. For the simulations described in this manuscript, L is set to 200 km - about the scale of Southern Ocean jet separation. γ is set to 1/120 days - long compared with

the typical eddy timescale but short enough for the fluxes to be fully diagnosed within the spinup period of these runs.

The traditional approach of simple damping (setting F to 0) leads to a steady state with a substantial persistent error. Instead, a mean flux is sometimes diagnosed by repeatedly averaging the damping flux of a run and then using it to adjust the mean flux for the next run. The method described here is qualitatively similar to a large number of such iterations.

References:

Arakawa, A., and Y.-J. G. Hsu, 1990: Energy conserving and potential-enstrophy dissipating schemes for the shallow water equations. *Mon. Wea. Rev.*, **109**, 18-36.

Best, S.E., V.O. Ivchenko, K.J. Richards, R.D. Smith, and R.C. Malone, 1999: Eddies in numerical models of the Antarctic Circumpolar Current and their influence on the mean flow, *J. Phys. Oceanogr*., **29**, 328-350.

Cunningham, S.A., S.G. Alderson, B.A. King and M.A. Brandon, 2003: Transport and variability of the Antarctic Circumpolar Current in Drake Passage, *J. Geophys. Res*, **108**, Art. 8084.

Doos, K. and D.J. Webb, 1994: The Deacon cell and the other meridional cells of the Southern Ocean, *J. Phys. Oceanogr.*, **24**, 429-442.

Doney, S.C., W.G. Large, and F.O. Bryan, 1998: Surface ocean fluxes and water mass transformations in the coupled NCAR climate system model, *J. Climate*, **11**, 1420-1441.

Ganachaud, A. and C. Wunsch, 2000: The oceanic meridional overturning circulation, mixing, bottom water formation, and heat transport, *Nature*, **408**, 453-457.

Gent, P., and J.C. McWilliams, 1990: Isopycnal mixing in ocean models, *J. Phys. Oceanogr*, **20**, 150-155.

_____, W.G. Large and F.O. Bryan, 2001: What sets the mean transport through Drake Passage?, *J. Geophys. Res.*, **106**(C2), 10.1029/2000JC900036, 2693-2712.

Gille, S.T., 1997: The Southern Ocean momentum balance: Evidence for topographic effects from numerical model output and altimeter data, *J. Phys. Oceanogr.*, **27**, 2219-2232.

Gnanadesikan, A., 1999: A simple theory for the structure of the oceanic pycnocline, *Science*, **283**,2077-2079.

_____, and R.W. Hallberg, 2000: The relationship of the Circumpolar Current to Southern Hemisphere winds in coarse-resolution ocean models, *J. Phys. Oceanogr.*, **30**, 2013-2034.

_____, R.D. Slater and B.L. Samuels, 2003: Dependence of oceanic heat transport and watermass transformation on subgridscale parameterization in coarse-resolution ocean models, *Geophys. Res. Lett.*, 30(18), 1967,doi:10.1029/2003GL018036.

Griffies, S.M., 1998: The Gent-McWilliams skew flux, *J. Phys. Oceanogr.*, **28**, 832-842.

_____, A. Gnanadesikan, R.C. Pacanowski, V.D. Larichev, R.D. Smith and J.K. Dukowicz, 1998: Isoneutral mixing in level-coordinate ocean models, *J. Phys. Oceanogr.*, **28**, 805-830.

_____., R.C. Pacanowski and R.W. Hallberg, 2000: Spurious diapycnal mxing associated with advection in a Z-coordinate ocean model, *Mon. Wea. Rev.*, **128**, 538-564.

Hallberg, R.W., 1997: Stable split time-stepping schemes for large-scale ocean modeling, *J. Comput. Phys.*, **135**, 946-952.

_____, 2000: Time-integration of diapycnal diffusion and Richardson-number dependent mixing in isopycnal coordinate ocean models, *Mon. Wea. Rev.*, **128**, 1402-1419.

_____, 2003: The suitability of large-scale ocean models for adapting parameterizations of boundary mixing and a description of a refined bulk mixed layer model, , *Proceedings 2003 A'ha Huliko'a Hawaiian Winter Workshop.* Muller and Henderson, Eds., 187-203.

_____, and A. Gnanadesikan, 2001: An exploration of the role of transient eddies in determining the transport of a zonally reentrant current, *J. Phys. Oceanogr.*, **31**, 3312-3330.

Held, I. M., and T. Schneider, 1999: The surface branch of the zonally averaged mass transport circulation in the troposphere. *J. Atmos. Sci.*, **56**, 1688-1697.

Huang, R.X. and J. Pedlosky, 1999: Climate variability inferred from a layered model of the ventilated thermocline, *J. Phys. Oceanogr.*, **29**, 779-790.

Johnson, G.C. and H. Bryden, 1989: On the strength of the Circumpolar Current, *Deep Sea. Res.*, **36,** 39-53.

Killworth, P.D. and M.M. Nanneh, 1994: Isopycnal momentum budget of the Antarctic Circumpolar Current in the Fine Resolution Antarctic Model, *J. Phys. Oceanogr.*, **24**, 1201-1233.

Kraus, E.B. and J.S. Turner, 1967: A one-dimensional model of the seasonal thermocline: II. The general theory and its consequences, *Tellus*, **19**, 98-106.

Lee, M.M. and A.Coward, 2003: Eddy mass transport for the Southern Ocean in an eddy-permitting global ocean model, *Ocean Modelling*, **5** (3): 249-266.

Marshall, J., D. Olbers, H. Ross and D. Wolf-Gladrow, 1993: Potential vorticity constraints on the dynamics and hydrography of the Southern Ocean, *J. Phys. Oceanogr.*, **23**, 465-487.

Marshall,J., and T. Radko, 2003: Residual-mean solutions for the Antarctic Circumpolar Current and its associated overturning circulation, *J. Phys. Oceanogr.*, **33**, 2341-2354.

Matsumoto, K. and 23 others, 2004: Evaluation of ocean carbon cycle models with data-based metrics, *Geophys. Res. Lett*., **31**, L07303, doi:10.1029/2003GL018970.

Nof, D., 2000: Does wind control the import and export of the South Atlantic? *J. Phys. Oceanogr.*, **30**, 2650-2667.

Redi, M., 1982: Oceanic isopycnal mixing by coordinate rotation, *J. Phys. Oceanogr.*, **12**, 1154-1158.

Renwick, J.A., Trends in the Southern Hemisphere polar vortex in NCEP and ECMWF reanalyses, Geophys. Res. Lett., 31, L07209, doi: 10.1029/2003GL19302,2004.

Rhines, P.B., 1977: The dynamics of unsteady currents, in *The Sea*, Vol. 6 *Marine modeling*, E. Goldberg, ed., Wiley, 189-318.

Sloyan, B. and S.R. Rintoul, 2001: Circulation, renewal and modification of Antarctic Mode and Intermediate Water, *J. Phys. Oceanogr.*, **31**, 1005-1030.

Smith, R.D., M.E. Maltrud, F.O. Bryan and M. W. Hecht, 2000: Numerical simulation of the North Atlantic Ocean at 1/10°, *J. Phys. Oceanogr.*, **30**, 1532-1561.

Smith, W.H.F and D.T. Sandwell, 1997: Global sea floor topography from satellite altimetry and ship depth soundings, *Science,* **277**, 1956-1962.

Speer, K.G., B. Sloyan, and S.R. Rintoul, 2000: The diabatic Deacon Cell,, *J. Phys. Oceanogr.*, **30**, 3212-3222.

Stammer, D., 1998: On eddy characteristics, eddy transports, and mean flow properties, *J. Phys. Oceanogr.*, **28**, 727-739.

Stevens, D.P. and V.O. Ivchenko, 1997: The zonal momentum balance in a realistic, eddy resolving general circulation model of the Southern Ocean, *Quart. J. Roy. Met. Soc.*, **123**, 929-951.

Talley, L.D., 1999: Simple coupled mid-latitude climate models, *J. Phys. Oceanogr.*, **29**, 2016-2037.

Talley, L.D., 2002: Shallow, intermediate and deep overturning components of the global heat budget, *J. Phys. Oceanogr.*, **33**, 530-560.

Tansley, C., and D. Marshall, 2001: On the dynamics of wind-driven circumpolar currents, *J. Phys. Oceanogr.*, **31**, 3258-3271.

Thompson, L., K. Kelly, D. Darr, and R. Hallberg, 2002: Buoyancy and Mixed Layer Effects on the Sea Surface Height Response in an Isopycnal Model of the North Pacific. *J. Phys. Oceanogr.*, **32**, 3657-3670.

Toggweiler, J.R., and H. Bjornsson, 2000: Drake Passage and paleoclimate, *J. Quart. Sci.*, **15**, 319-328.

_____, and B.L. Samuels, 1993: New radiocarbon constraints on the upwelling of abyssal water to the ocean's surface, in *The Global Carbon Cycle*, M. Heimann, ed., Springer-Verlag, 333-365.

_____, and B.L. Samuels, 1995: Effect of Drake Passage on the global thermohaline circulation, *Deep Sea Res., Part I*, **42**, 477-500.

_____, and _____, 1998: On the ocean's large-scale circulation near the limit of no vertical mixing, *J. Phys. Oceanogr.*, **28**, 1832-1852.

Trenberth, K. E., and J. M. Caron, 2001: Estimates of Meridional Atmosphere and Ocean Heat Transports. *J. Clim.*, **14**, 3433-3443.

Veronis, G., 1996: Effect of a constant, zonal wind on wind-driven ocean circulation, *J. Phys. Oceanogr.*, **26**, 2525-2528.

Visbeck, M., J. Marshall, T. Haine, and M. Spall 1997: Specification of Eddy Transfer Coefficients in Coarse-Resolution Ocean Circulation Models. Journal of Physical Oceanography. **27**,. 381-402.

Warren, B., J. LaCasce and P.A. Robbins, 1996: On the obscurantist physics of "form drag" in theorizing about the Circumpolar Current, *J. Phys. Oceanogr.*, **26**, 2297-2301.

Whitworth, T. III, W.D. Nowlin and S.J. Worley, 1982: The net transport of the Antarctic Circumpolar Current through Drake Passage, *J. Phys. Oceanogr.*, **12**, 960-971.

Young, W.R.. 1994: The Subinertial Mixed Layer Approximation. *J. Phys. Oceanogr.*, **24**, 1812-1826.

Zhang, Y.X. and A.J. Semtner, 2001: The Antarctic Circumpolar Wave in a global, high-resolution, coupled ice-ocean model, *Ann. Glaciology*, **33**, 539-544.

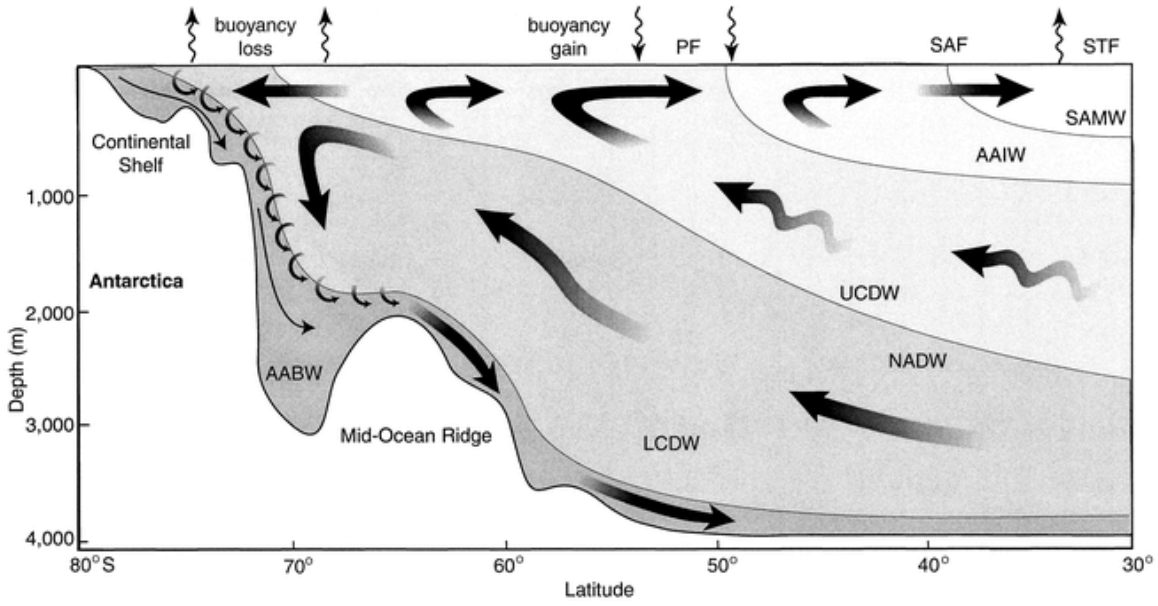

Figure 1: Schematic of the hypothesized circulation in the Southern Ocean from Speer et al., (2000).

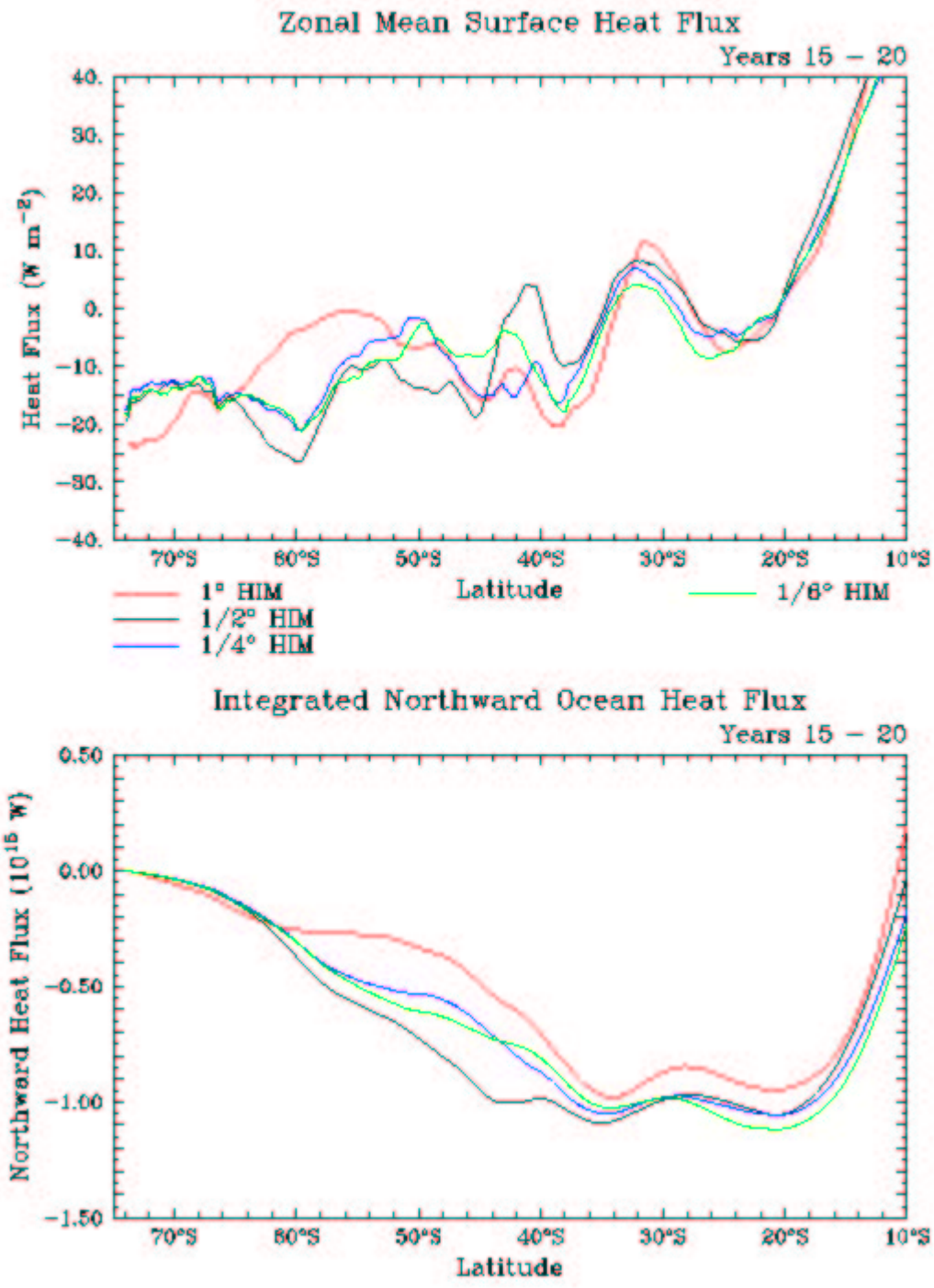

Figure 2: Heat fluxes and transport at different model resolutions.

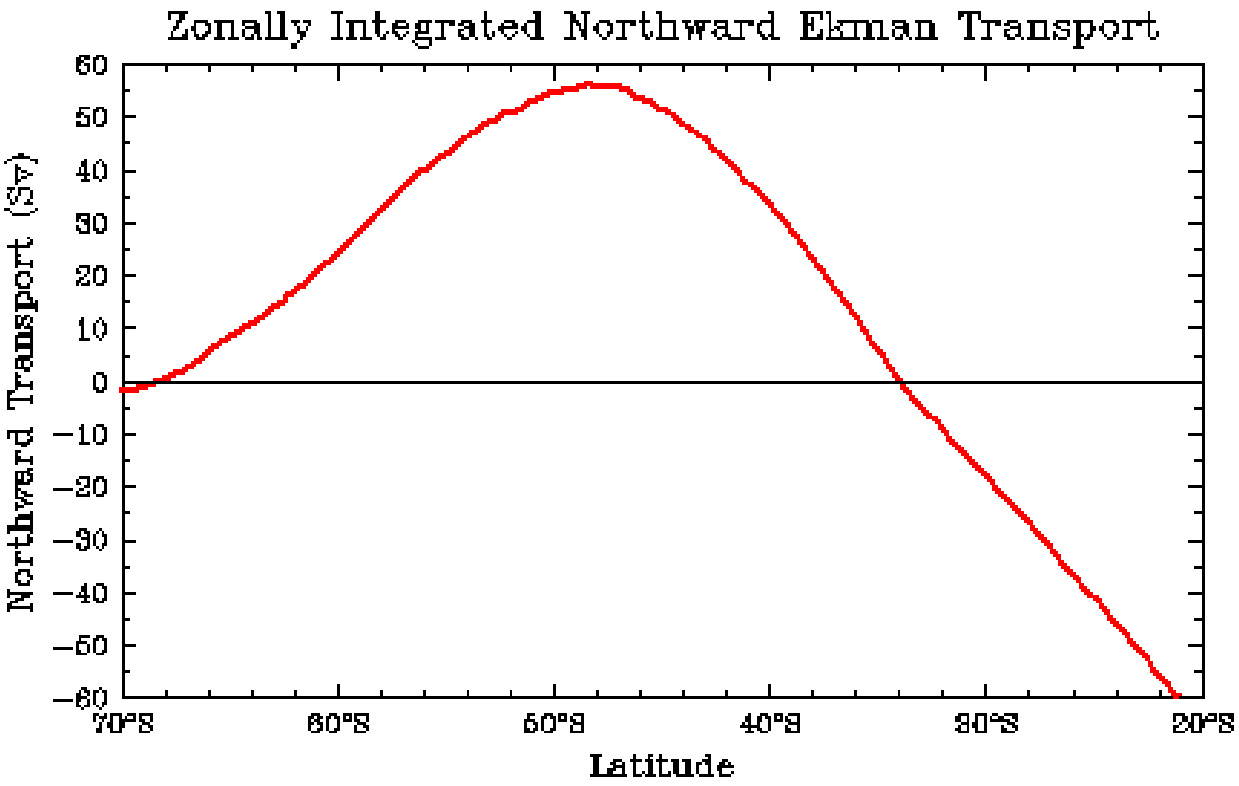

Figure 3: Zonally integrated northward Ekman transport $\int(\tau/\rho_o f)dx$ in the base run. In the high wind runs this transport is increased by 20%. In the low wind runs it is decreased by 20%.

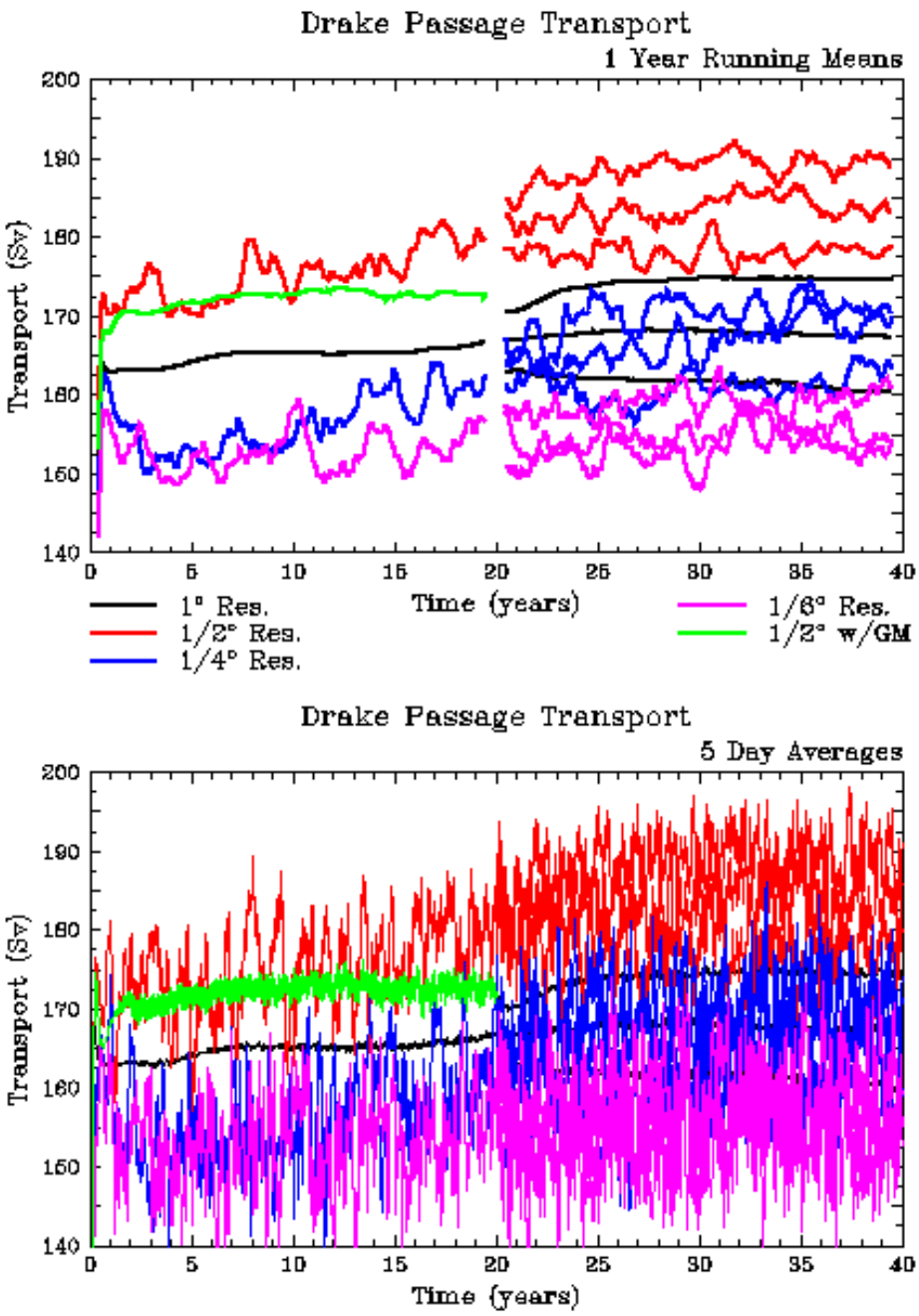

Figure 4: Drake Passage transport at 1º (black), 1/2º (red), 1/4º (blue) and 1/6º (magenta) resolution. Green lines show simulation at 1/2º resolution with GM parameterization turned on, suppressing the eddy field. Top panel: 1 year running means, bottom panel, 5 day averages.

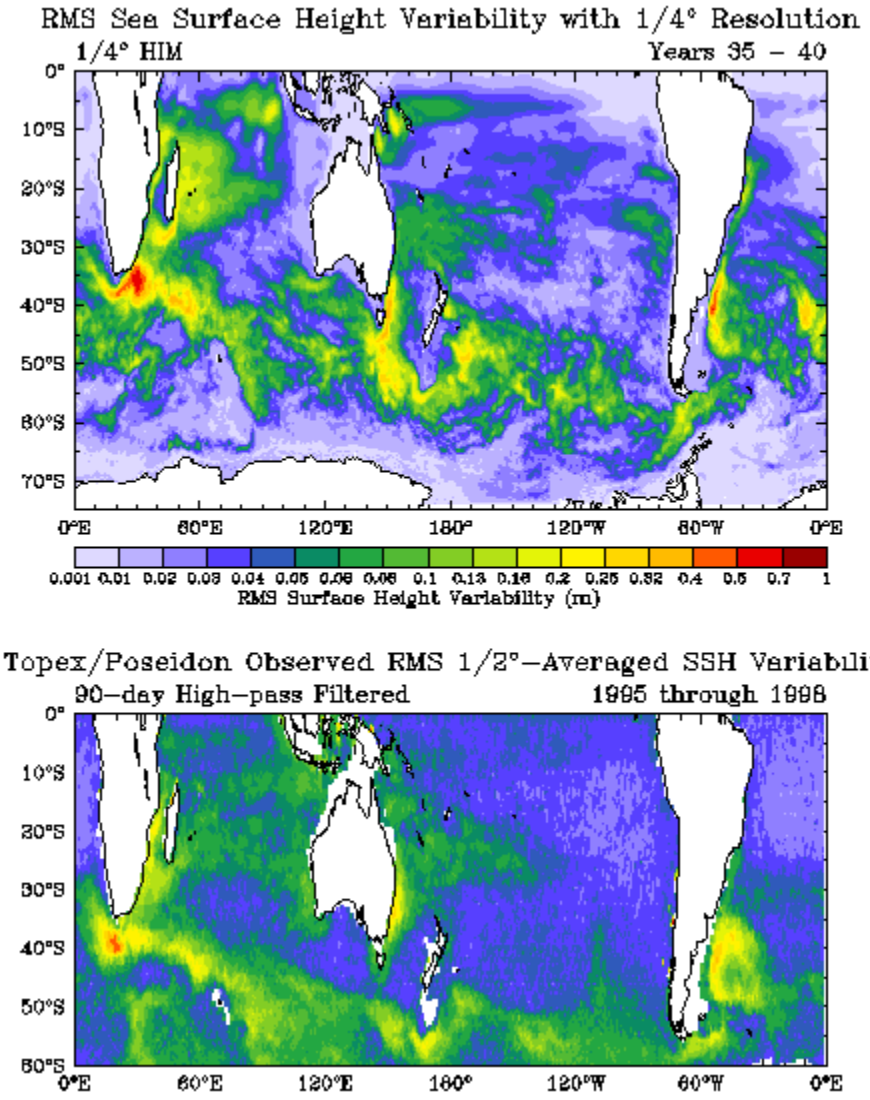

Figure 5: RMS SSH in the models and from TOPEX. Upper left: ¼°model with middle winds from years 35-40. Bottom left: TOPEX Poseidon SSH anomalies on a 1/2° grid, 90-day highpass-filtered to remove the seasonal cycle. Upper right: Same as upper left but for 1/6°, years 15-20. Lower left: Same as upper left but for 1/6°, years 35-40.

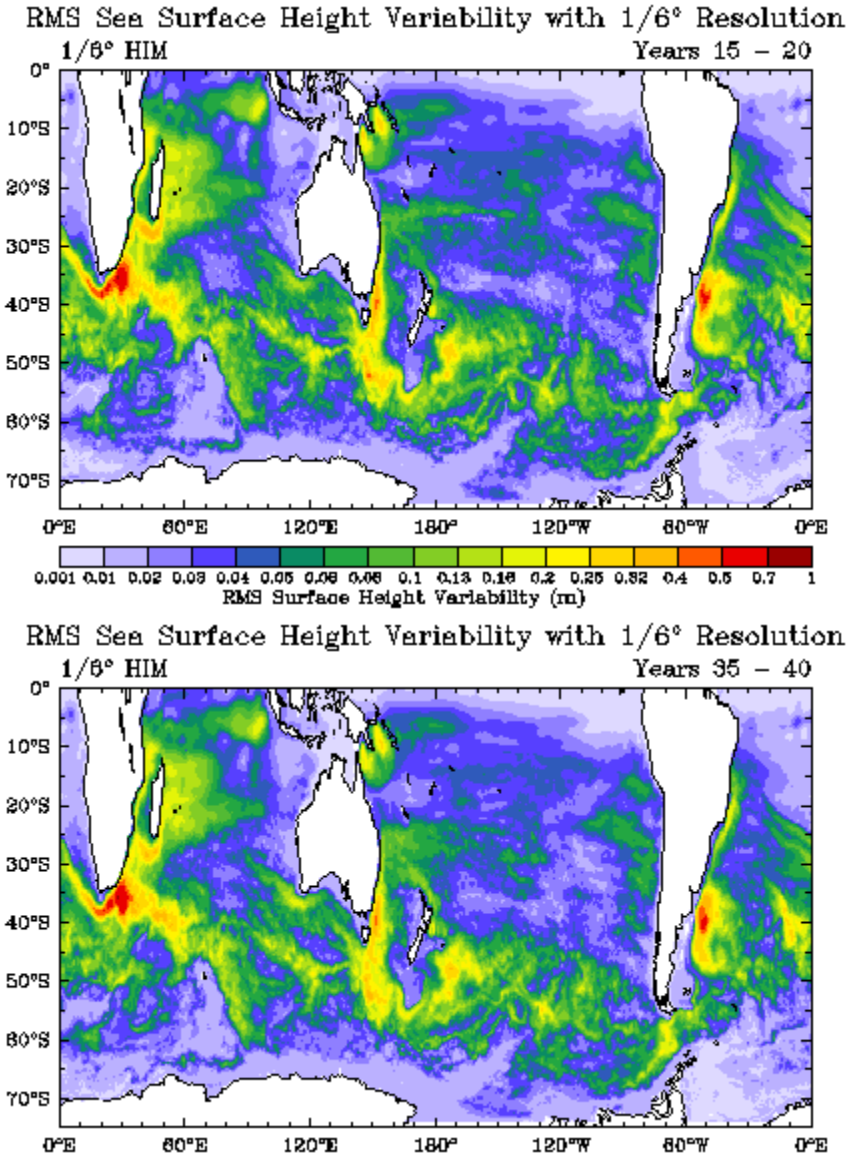

Figure 5 (continued)

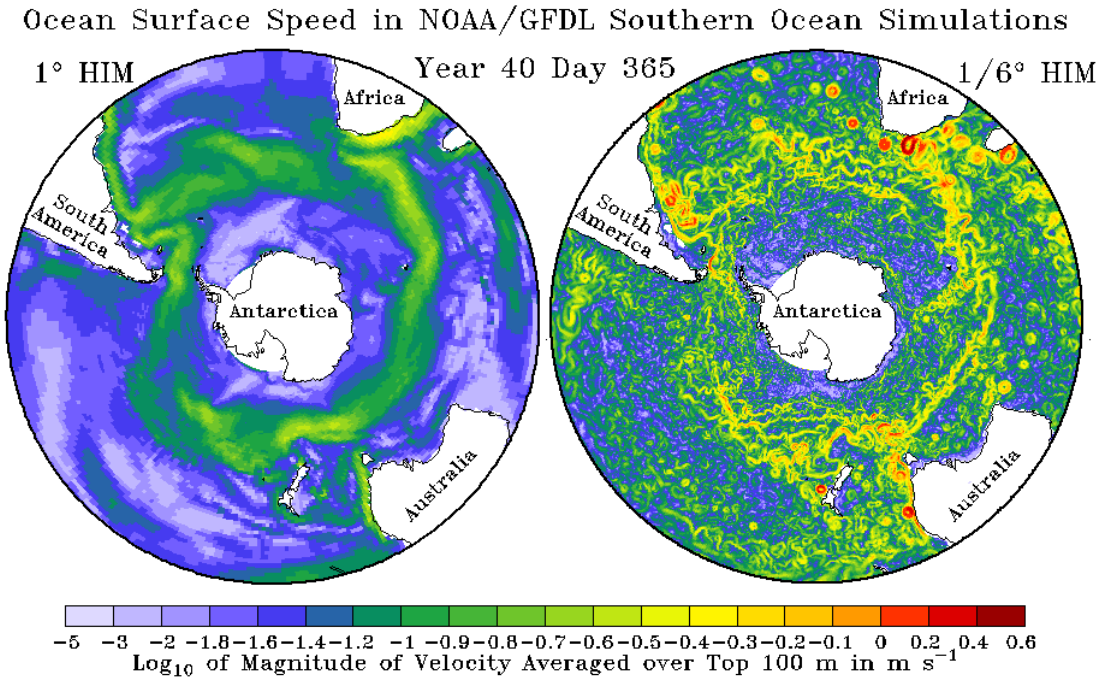

Figure 6: Surface speed in 1º and 1/6º models at the same point in time. Note that the large-scale structure of the 1º model is quite similar to the 1/6º model (currents are located in similar locations and have similar horizontal extents). The main difference is in the presence of intense jets and eddies in the 1/6º model.

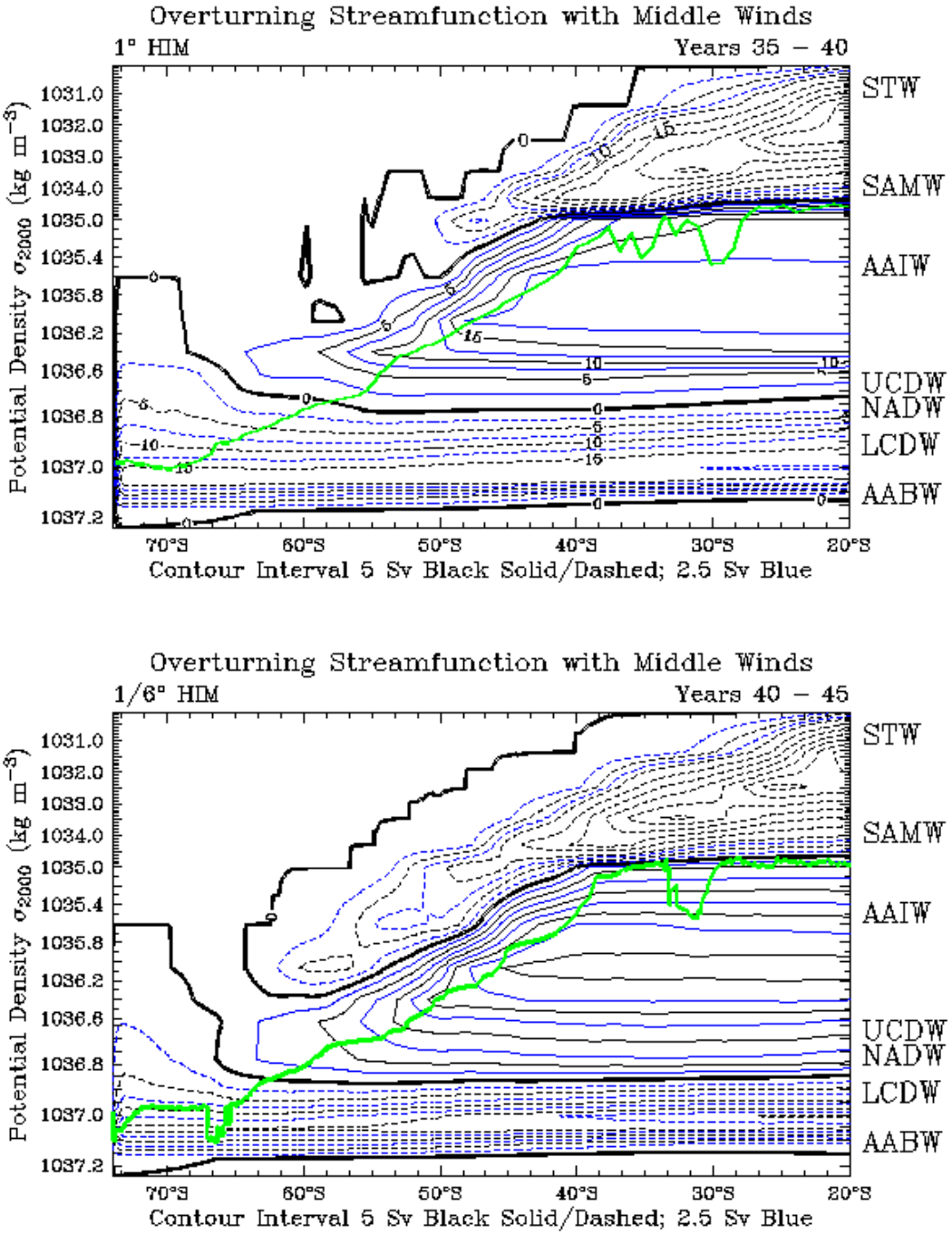

Figure 7: Overturning streamfunction at 1 and 1/6º resolution in density space. Positive values (solid lines) indicate cells that flow clockwise, while negative vales (dashed lines) flow counterclockwise. Green lines show zonal maximum time-averaged density in top 50m. Circulation above this level can have contributions from the mixed layer. Watermasses (as in Figure 1 with the addition of STW, subtropical water) are shown at right.

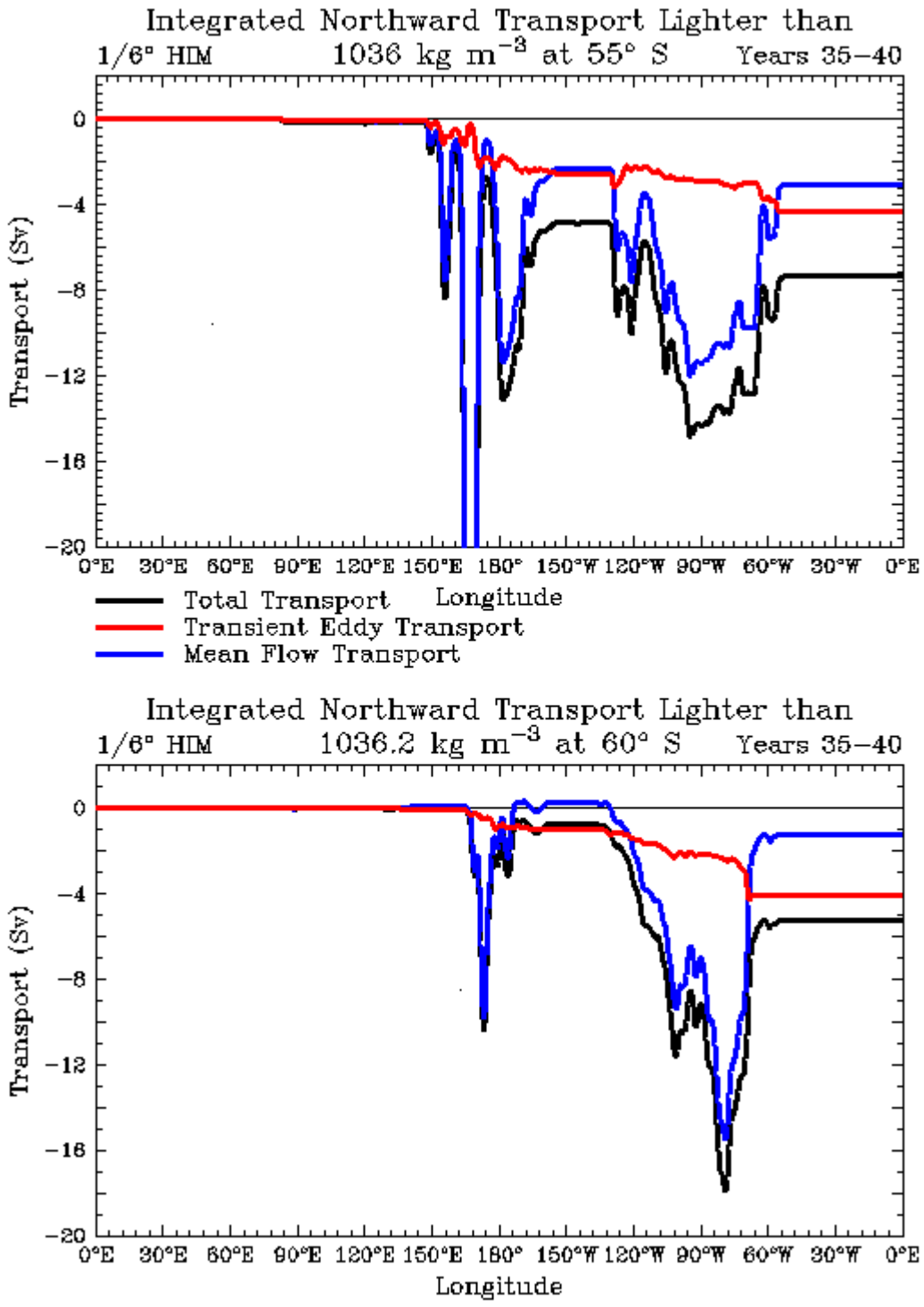

Figure 8: Breakdown of flow of light water into time-mean and transient eddy components.

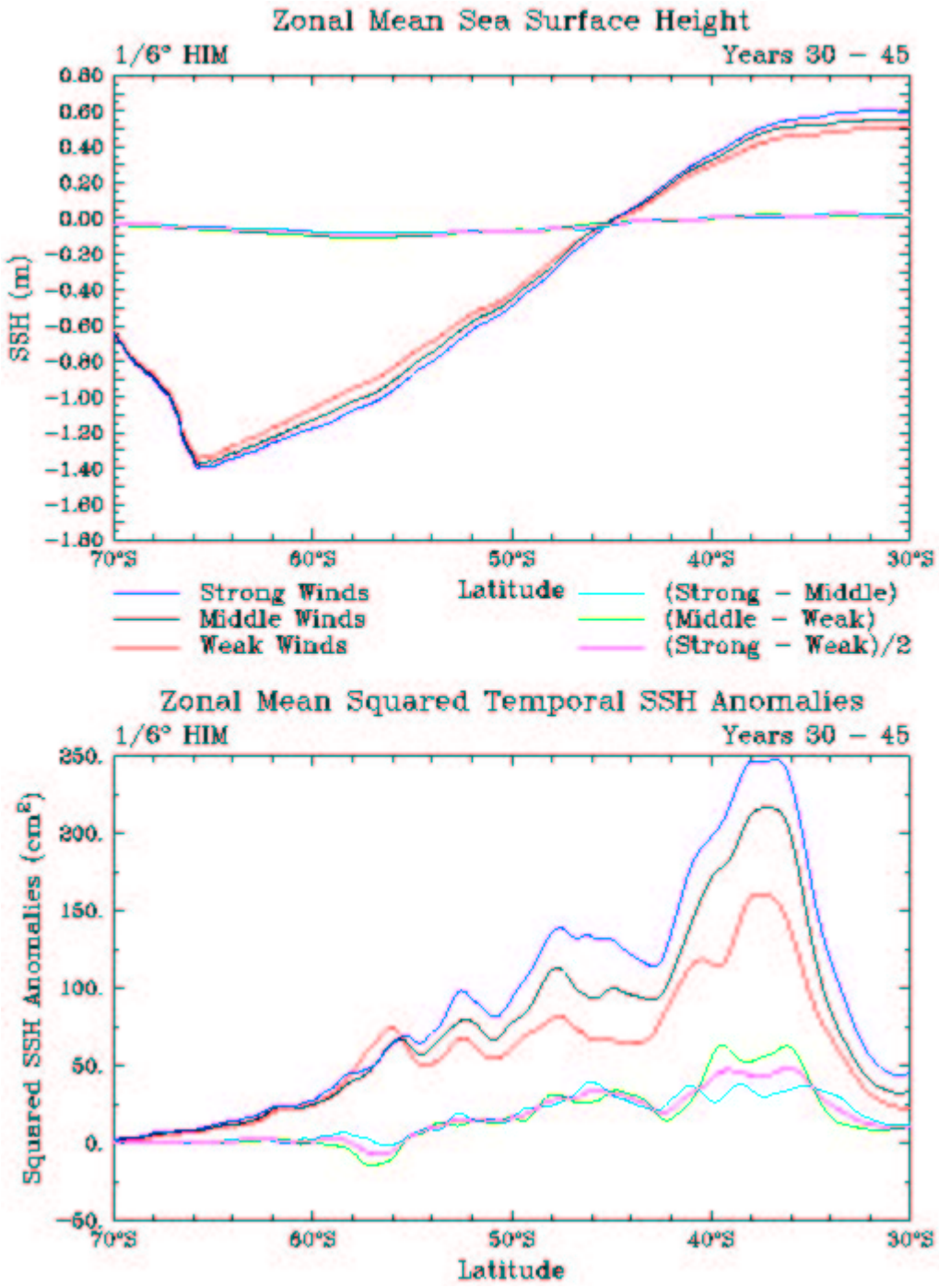

Figure 9: Sea surface height responses to changing winds. Top: Zonal mean SSH, showing that the changes are small in comparison with the 2 m drop across the ACC. change in mean square SSH anomalies resulting from changes in winds. Changes are essentially linear in the wind stress.

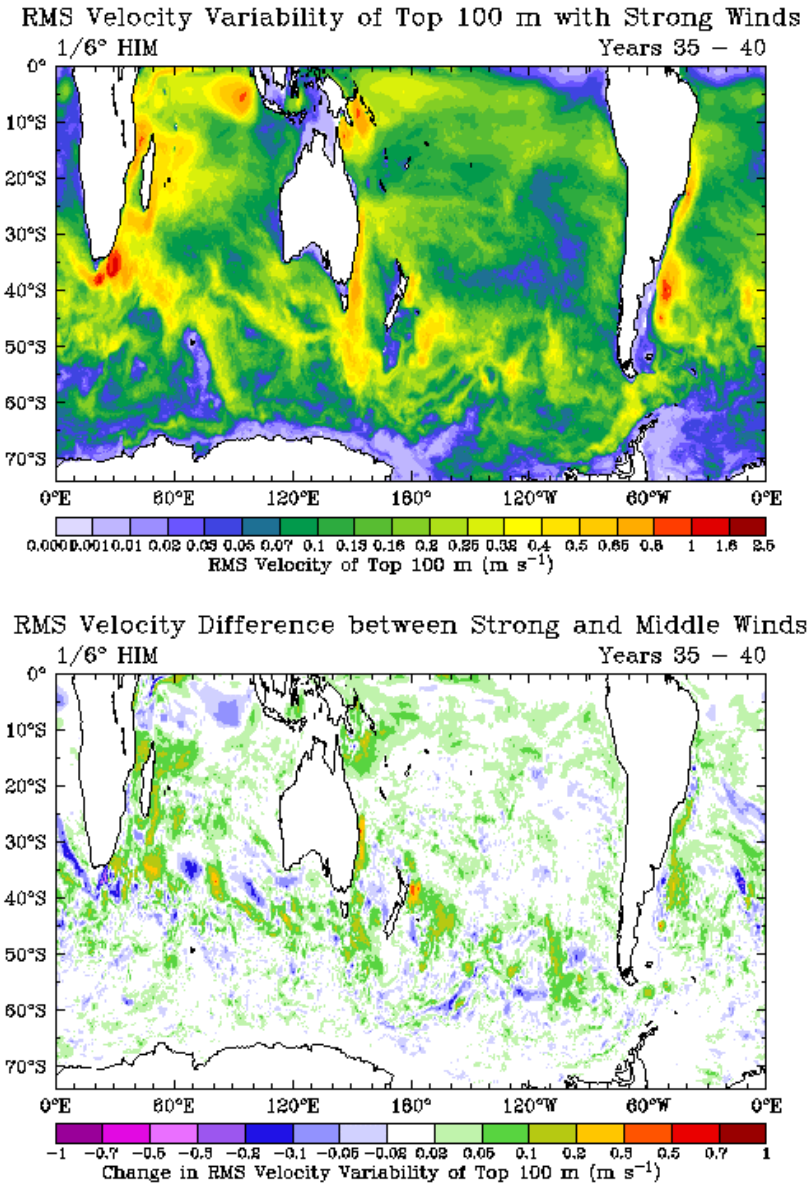

Figure 10: Change in surface velocity variance from changing winds.

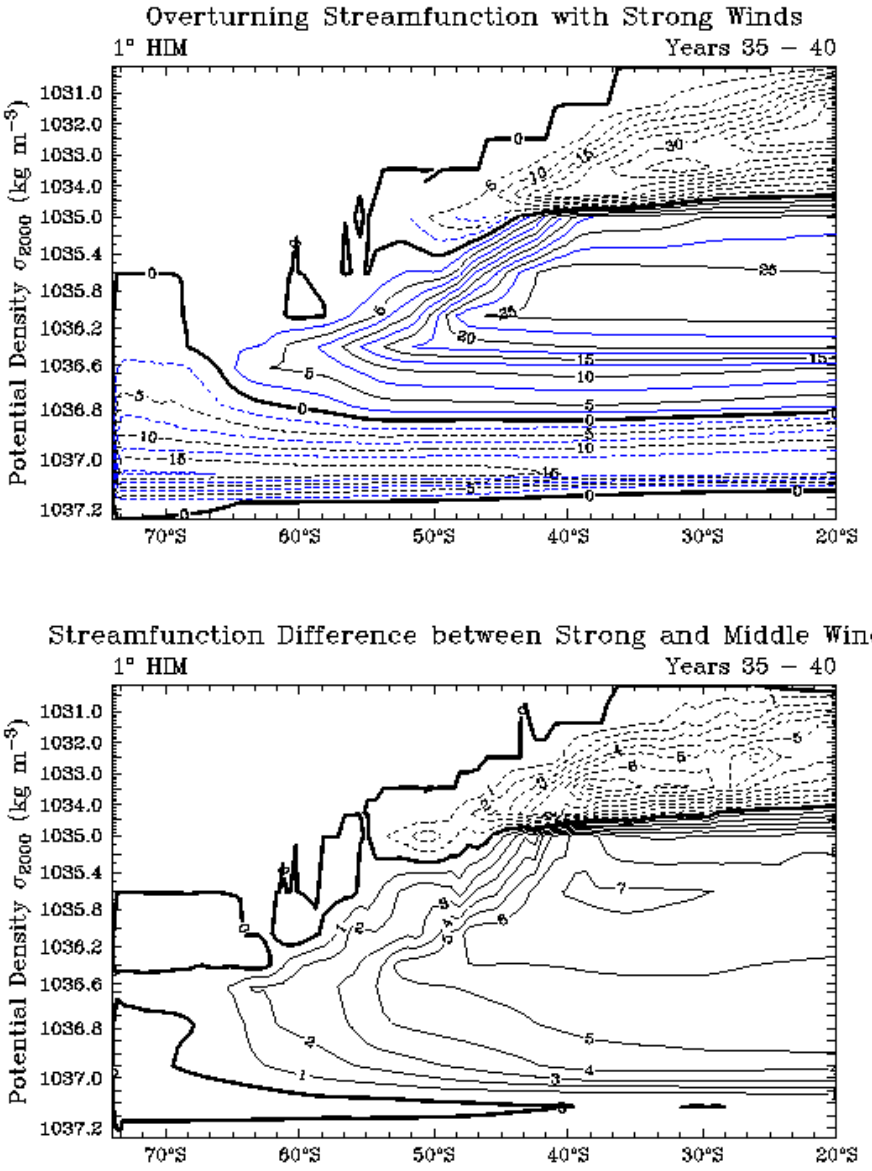

Figure 11: Overturning streamfunction in Density space. (A) Overturning streamfunction, strong winds, 1º. (B) Difference between overturning streamfunction with strong and middle winds, 1º. (C) Same as A, but at 1/6º resolution. (D) Same as B but at 1/6º resolution. Both (B) and (D) use the same 1 Sv contour interval, while (A) and (C) use a 2.5 Sv interval.

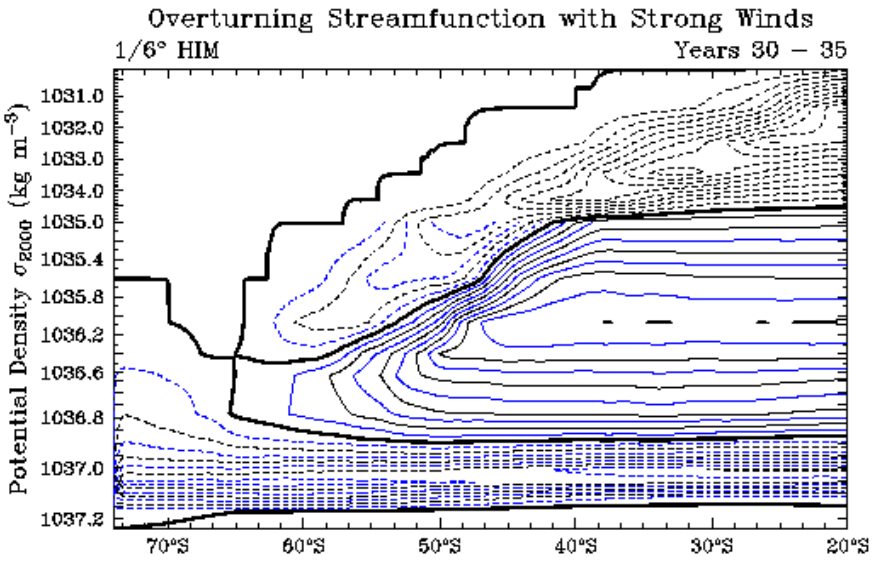

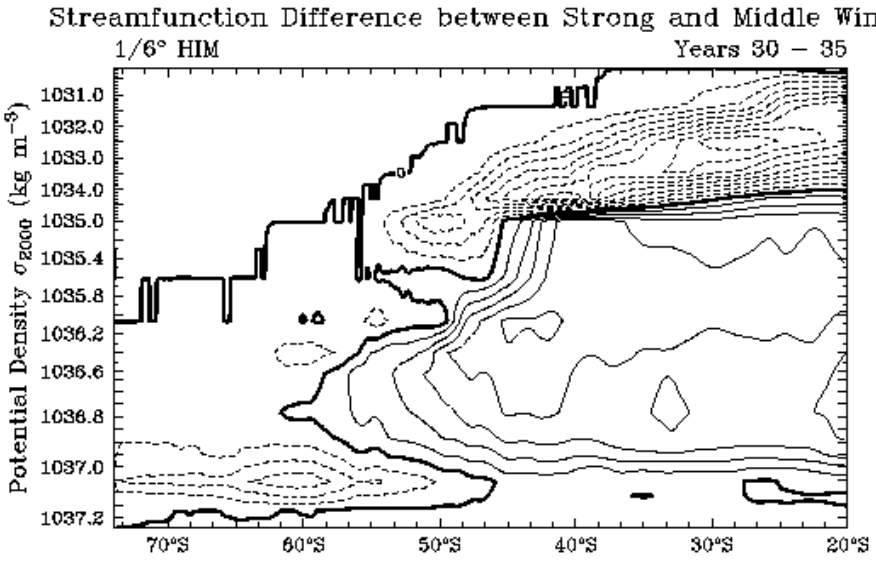

Figure 11 (continued)

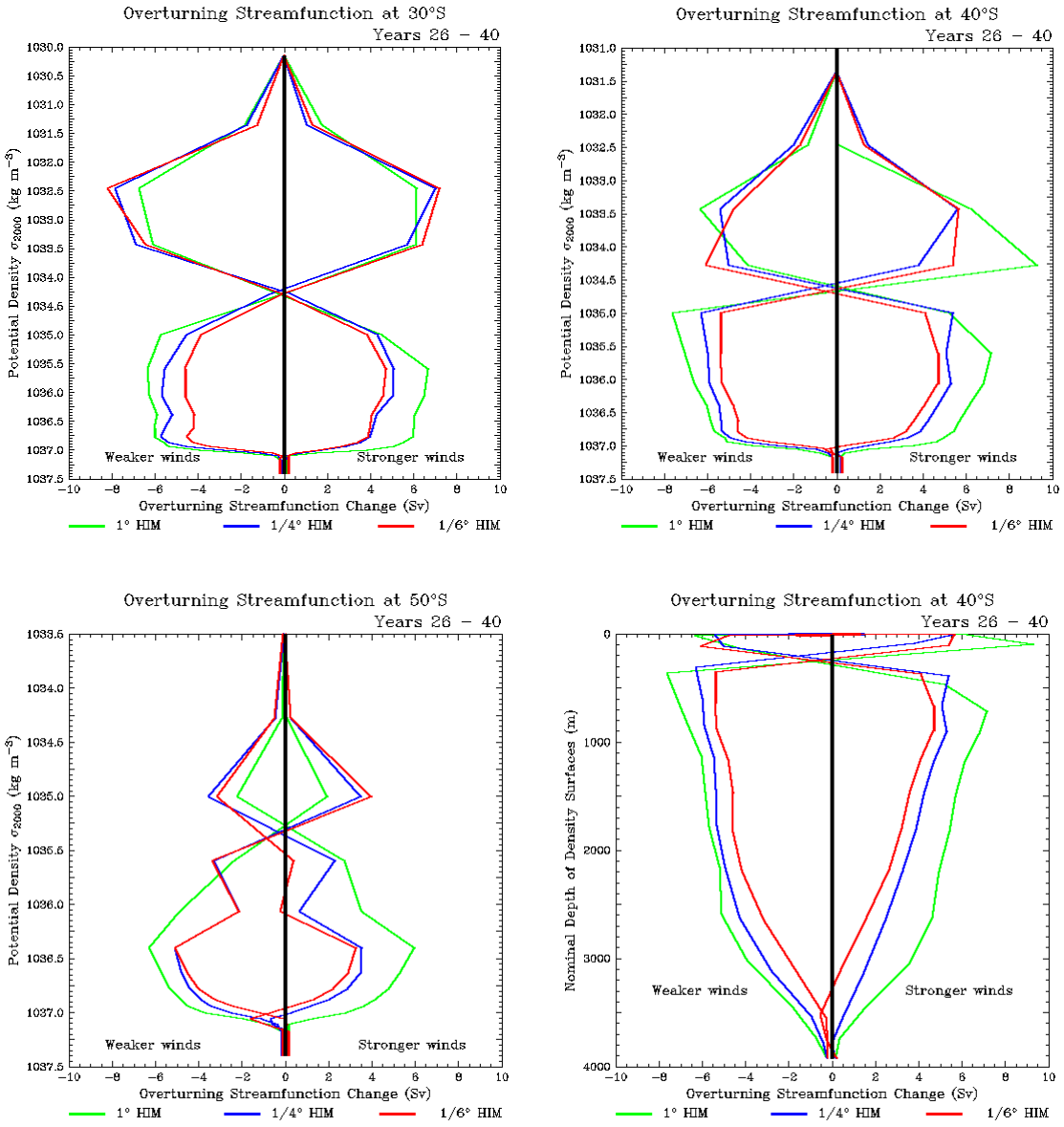

Figure 12: Zonally integrated overturning changes in density space at latitudes of 30°S (A), 40°S (B), and 50°S (C) and resolutions of 1° (green), ¼° (blue), and 1/6° (red). The changes for both increasing and decreasing winds are shown in this figure; the increasing winds are the "S" shaped curves, while the decreasing winds are the reverse. (D) Same but with the overturning remapped to the average depth of the density surface.